

Supplementary Information

for the article

Electrostatic complementarity in pseudoreceptor modeling based on drug molecule crystal structures: the case of loxistatin acid (E64c)

Ming W. Shi,^a Alexandre N. Sobolev,^a Tanja Schirmeister,^b Bernd Engels,^c Thomas C. Schmidt,^c Peter Luger,^d Stefan Mebs,^d Birger Dittrich,^e Yu-Sheng Chen,^f Joanna M. Bąk,^a Dylan Jayatilaka,^a Charles S. Bond,^a Michael J. Turner,^a Scott G. Stewart,^a Mark A. Spackman,^a and Simon Grabowsky^{a,g,*}

^a The University of Western Australia, School of Chemistry and Biochemistry, M310, 35 Stirling Highway, Crawley WA 6009, Australia.

^b Johannes-Gutenberg-Universität Mainz, Institut für Pharmazie und Biochemie, Staudinger Weg 5, 55128 Mainz, Germany.

^c Julius-Maximilians-Universität Würzburg, Institut für Physikalische und Theoretische Chemie, Emil-Fischer-Str. 42, 97074 Würzburg, Germany.

^d Freie Universität Berlin, Institut für Chemie und Biochemie, Fabeckstr. 36a, 14195 Berlin, Germany.

^e Universität Hamburg, Institut für Anorganische und Angewandte Chemie, Martin-Luther-King-Platz 6, 20146 Hamburg, Germany.

^f ChemMatCARS, Center for Advanced Radiation Sources, c/o Advanced Photon Source/ ANL, The University of Chicago, 9700 South Cass Avenue, Bldg. 434D, Argonne, Illinois 60439, U.S.A.

^g Universität Bremen, Fachbereich 2 – Biologie/Chemie, Leobener Str. NW2, 28359 Bremen, Germany.

*E-Mail: simon.grabowsky@uni-bremen.de.

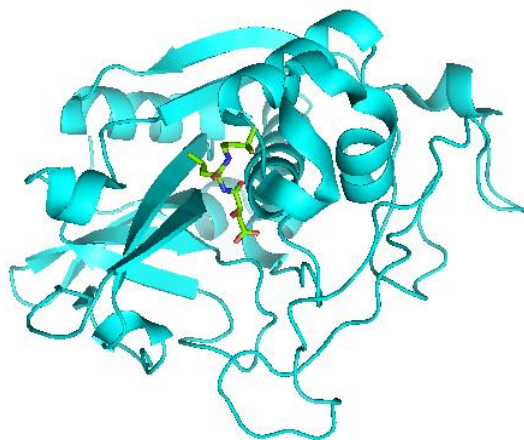


Figure S1. PyMOL generated structure of the cathepsin B-E64c complex from the crystal structure with PDB code 1ITO^{3c}.

Table S1. Crystallographic details.

E64c			
Chemical formula	C ₁₅ H ₂₆ N ₂ O ₅	μ/mm^{-1}	0.034
M/g.mol-1	314.38	Crystal size/mm ³	0.16 x 0.11 x 0.02
Crystal system	triclinic	Beamline	APS, 15-ID-B
Space group	P1	T/K	12
Z	4	Wavelength/Å	0.3936
a/Å	10.036(2)	Min./max. θ/°	1.68/16.41
b/Å	11.838(2)	sinθ _{max} /λ/Å ⁻¹	0.72
c/Å	15.884(3)	d/Å	0.70
α/°	79.36(3)	No. of collected reflections	80246
β/°	78.98(3)	No. of unique reflections	9541
γ/°	74.71(3)	No. of observed refl. $F \geq 4\sigma(F)$	8764
V/Å ³	1768.7(6)	Redundancy	8.41
$\rho_x/\text{g cm}^{-3}$	1.181	Completeness /%	87.0
F(000)	680	R _{int} /%	8.09
Spherical refinement		Invariom refinement	
R(F) /%	10.99	R(F) (%)	10.23
wR(F ²) /%	26.79	wR(F ²) (%)	19.74
GooF	1.10	GooF	7.94
Min/max δ _{res} ρ /e·Å ⁻³	-0.47/0.81	Min/max δ _{res} ρ /e·Å ⁻³	-0.45/0.68

Table S2. Selected bond distances (\AA) and angles ($^{\circ}$) of the four molecules (A to D) in the asymmetric unit of the E64c crystal structure and of the optimized geometry (opt).

Distance	A	B	C	D	opt
C1-C2	1.488(9)	1.473(9)	1.469(9)	1.473(9)	1.479
C1-O1	1.429(7)	1.409(8)	1.406(8)	1.421(8)	1.428
C2-O1	1.429(8)	1.409(7)	1.413(8)	1.419(7)	1.427
C2-C3	1.508(9)	1.504(9)	1.488(9)	1.497(9)	1.502
C1-C4	1.494(8)	1.496(9)	1.509(8)	1.494(8)	1.512
C3-O2	1.207(7)	1.211(8)	1.220(7)	1.216(8)	1.200
C3-O3	1.309(8)	1.315(8)	1.320(7)	1.308(8)	1.351
C4-N1	1.333(8)	1.336(8)	1.336(8)	1.344(8)	1.354
C4-O4	1.234(8)	1.229(8)	1.236(8)	1.231(8)	1.218
Angle					
C1-O1-C2	62.8(4)	63.0(4)	62.8(4)	62.5(4)	62.4
O1-C1-C2	58.6(4)	58.5(4)	58.8(4)	58.7(4)	58.8
O1-C2-C1	58.6(4)	58.5(4)	58.4(4)	58.9(4)	58.8
O1-C2-C3	115.6(5)	116.6(5)	116.4(5)	116.8(5)	115.6
O1-C1-C4	117.1(5)	117.3(5)	117.1(5)	117.4(5)	118.5

Table S3. Selected torsion angles ($^{\circ}$) of the four molecules (A to D) in the asymmetric unit of the E64c crystal structure, of the optimized geometry (opt), of the reversible (rev) and the irreversible (irr) cathepsin B – E64c complex.

Torsion angle	A	B	C	D	opt	rev	irr
C3-C2-C1-C4	148.0(6)	147.0(5)	147.9(5)	147.2(5)	118.3	156.3	178.1
C1-C4-N1-C5	172.6(5)	173.7(5)	172.6(5)	171.3(5)	114.7	-157.1	-179.6
N1-C5-C7-C8	-56.4(7)	-48.9(9)* -69.4(12)*	-54.8(7) -51.9(7)	111.7 -173.9	-173.9 -107.0	-173.9 -107.0	-107.0
N1-C5-C6-N2	157.8(5)						
		157.4(6)	161.4(5)	156.9(5)	115.8	99.8	114.1

* Two disorder components in molecule B.

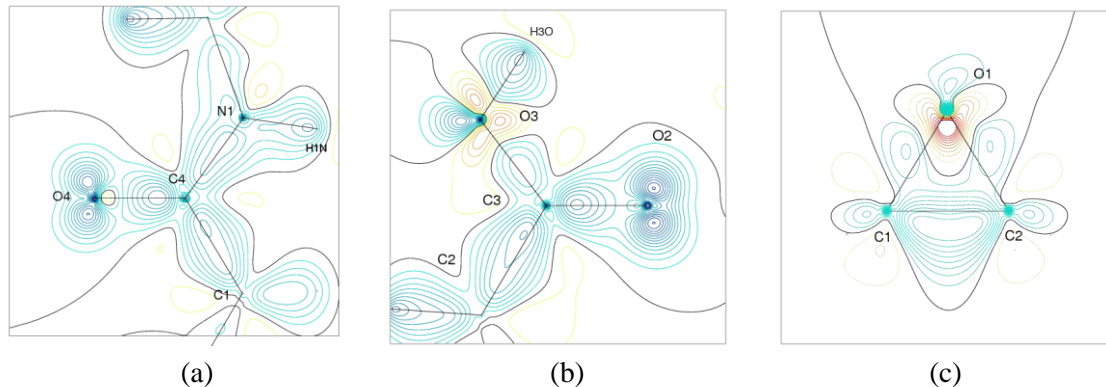


Figure S2. Static deformation density maps of E64c after invariom refinement. (a) Amide group, (b) carboxylic acid group, (c) epoxide ring. Contour interval: $0.05 \text{ e}\text{\AA}^{-3}$, blue = positive, red = negative.

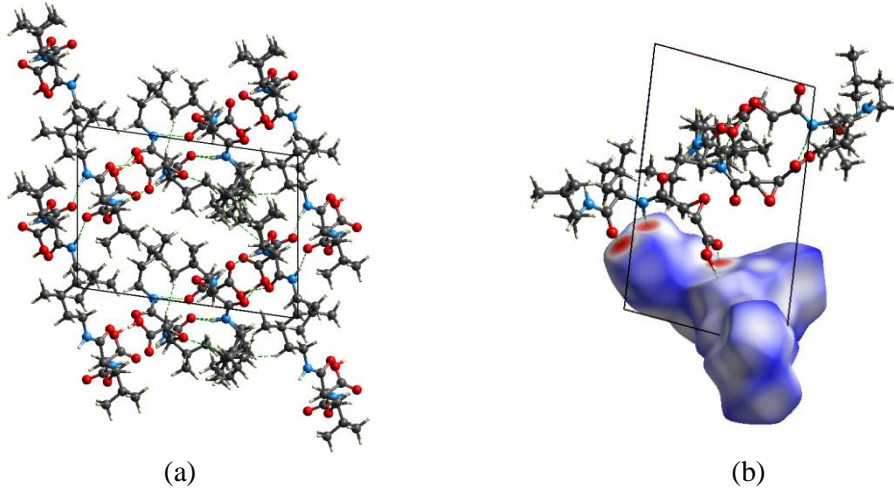


Figure S3. (a) Unit cell projection of E64c down the a -axis. (b) Unit cell projection of E64c down the b -axis, including a Hirshfeld surface of molecule D with d_{norm} mapped onto it. Colour code of d_{norm} on the Hirshfeld surface: -0.801 to 1.761.

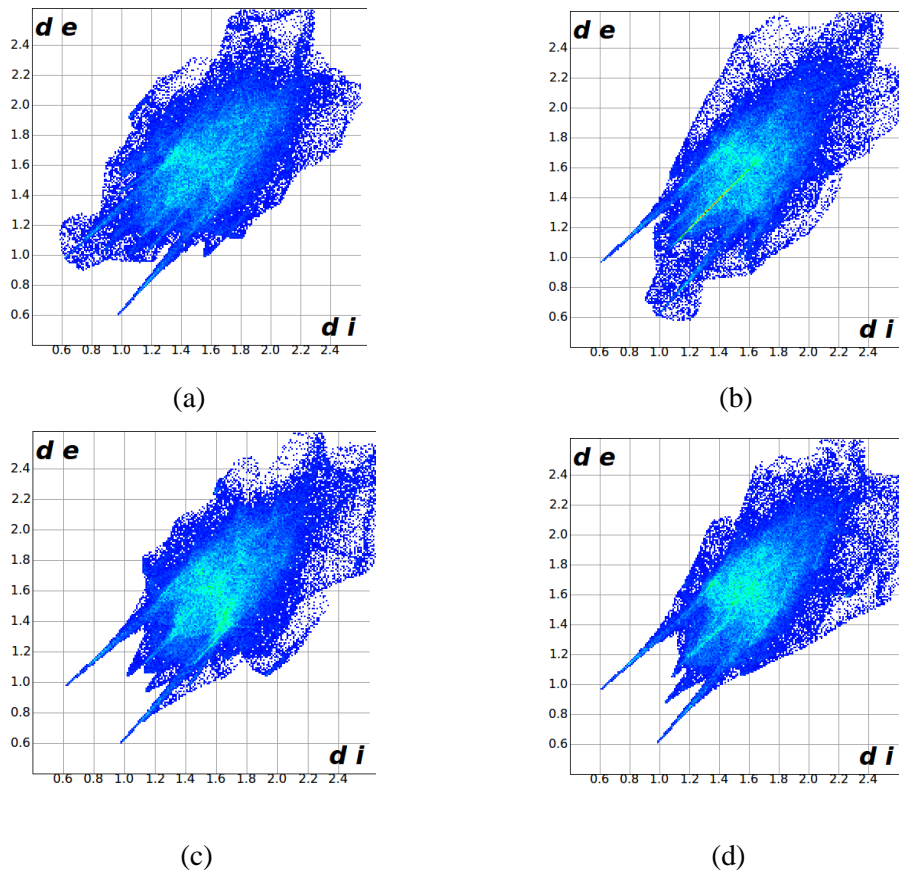
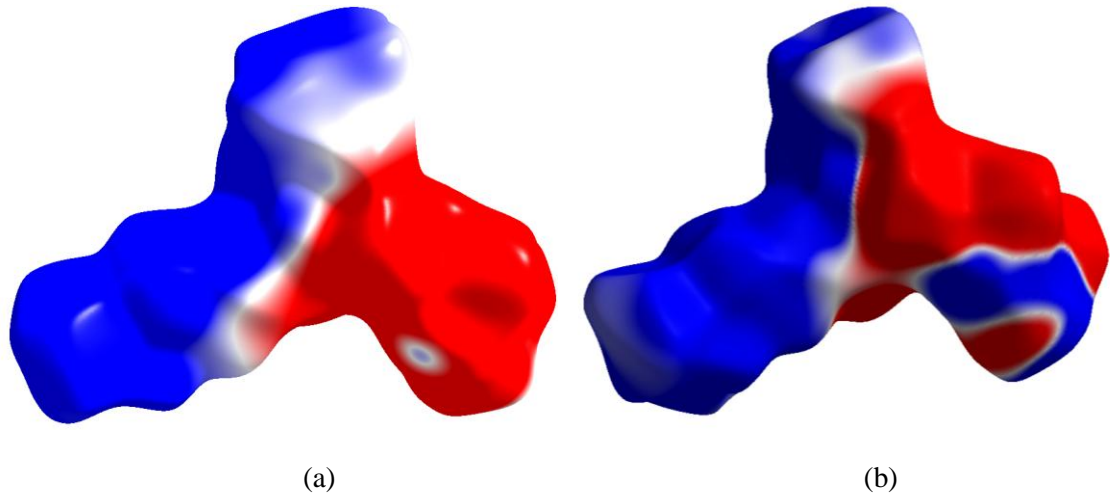


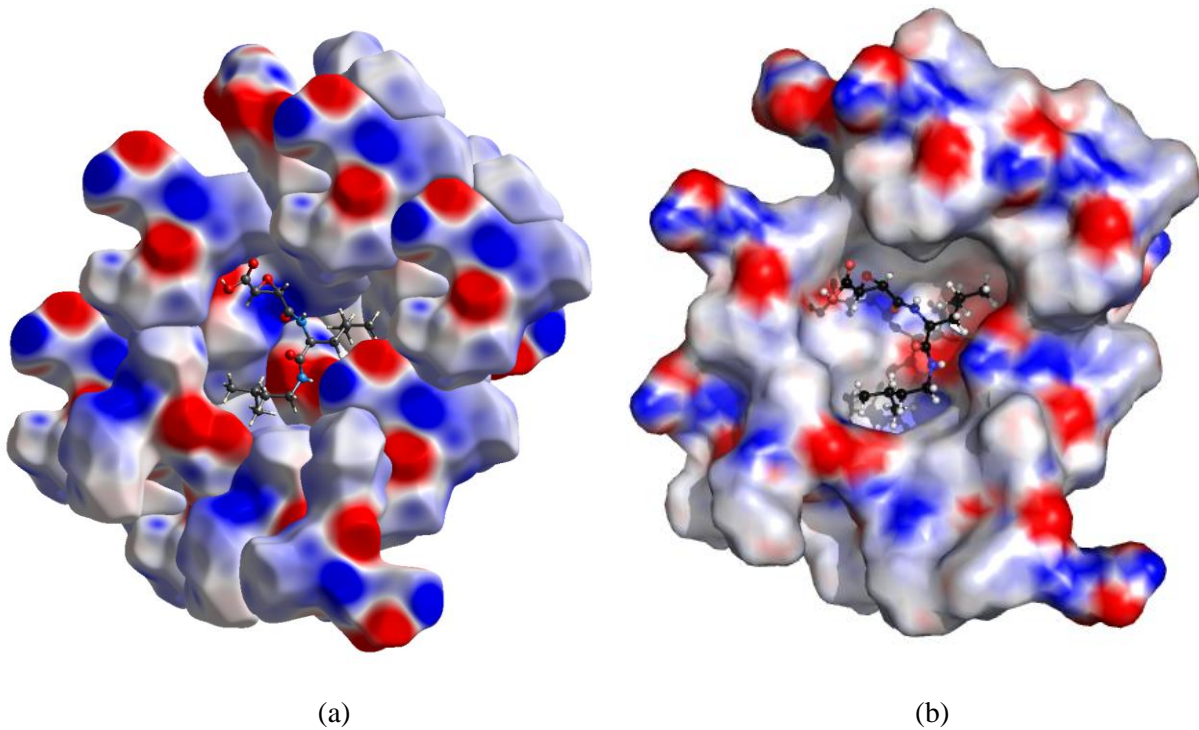
Figure S4. Fingerprint plots of the four symmetry-independent molecules A to D [(a) – (d)] of the E64c crystal structure derived from their Hirshfeld surfaces.



(a)

(b)

Figure S5. Hirshfeld surfaces of molecule D with corresponding electrostatic potentials mapped onto them derived from (a) the invariom approach and (b) a single-point ab-initio calculation (HF/6-31G(d)). Colour code: ± 0.01 au.



(a)

(b)

Figure S6. A cluster of E64c molecules in the molecular crystal around a central E64c molecule. (a) Individual Hirshfeld surfaces with single-point ab-initio electrostatic potentials mapped onto them (HF/6-31G(d)); colour code: ± 0.05 au. (b) Connolly surface with APBS-derived electrostatic potential mapped onto it; colour code: $\pm 5kT/e$.

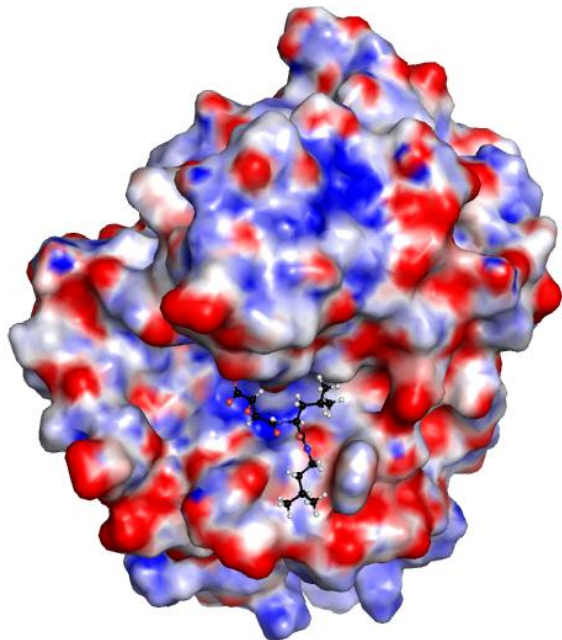


Figure S7. Connolly surface of the reversible cathepsin B – E64c complex with an APBS-derived electrostatic potential mapped onto it; colour code: $\pm 20\text{kT/e}$.

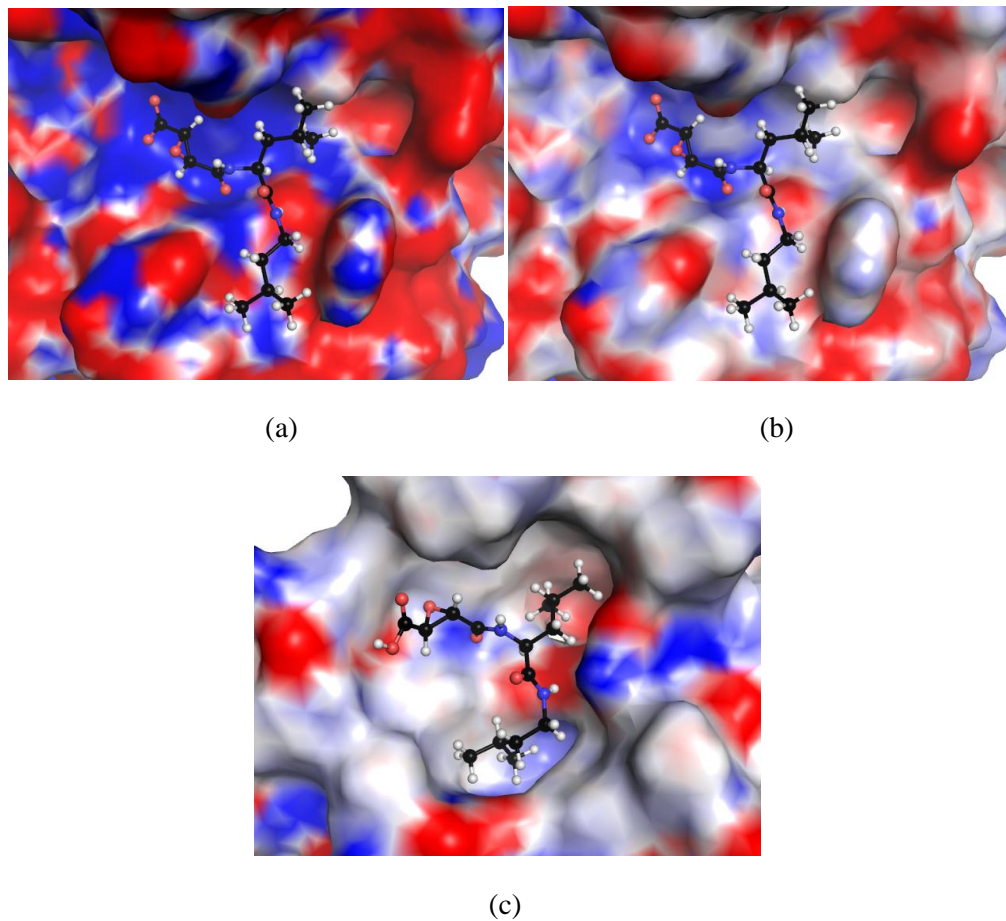


Figure S8. (a), (b) Detail of Figure S7 with different colour scale: $\pm 5\text{kT/e}$ in (a), $\pm 20\text{kT/e}$ in (b).
(c) Detail of Figure S6b with colour scale $\pm 5\text{kT/e}$.

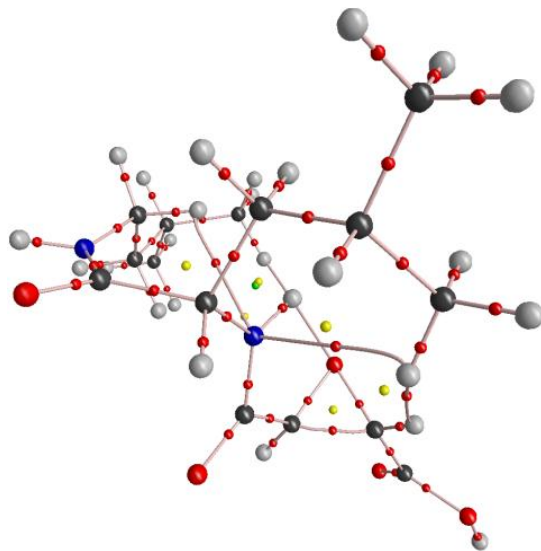


Figure S9. Molecular graph of E64c at its theoretically optimized geometry according to the Quantum Theory of Atoms in Molecules. Red = bond critical points; yellow = ring critical points; green = cage critical point.

Table S4. Atomic properties of E64c according to the Quantum Theory of Atoms in Molecules at the experimental geometry derived from the invariom approach (inv, molecule D) and at the optimized geometry derived from the theoretical wavefunction at B3LYP/6-311++G(2d,2p) level of theory (opt). Charge Q (in e), volume V (\AA^3) cut at an electron-density isovalue of 0.001 au.

	Q		V	
	inv	opt	inv	opt
O1	-0.80	-0.88	15.50	16.30
O2	-0.94	-1.13	16.44	19.89
O3	-1.08	-1.08	16.79	17.97
O4	-0.91	-1.13	16.28	20.31
N1	-0.97	-1.03	12.01	11.98
C1	0.27	0.38	8.43	8.32
C2	0.26	0.39	8.72	8.31
C3	1.33	1.55	6.28	5.48
C4	1.08	1.38	6.93	5.90
H1	0.08	0.08	6.11	6.57
H2	0.08	0.06	6.03	6.92

Table S5. Bond-topological properties of E64c according to the Quantum Theory of Atoms in Molecules at the experimental geometry derived from the invariom approach (inv, molecule D) and at the optimized geometry derived from the theoretical wavefunction at B3LYP/6-311++G(2d,2p) level of theory (opt). Electron density (ρ in $e\text{\AA}^{-3}$), Laplacian of the electron density ($\nabla^2\rho$ in $e/\text{\AA}^{-5}$) and ellipticity (ε) at selected bond critical points.

	ρ		$\nabla^2\rho$		ε	
	inv	opt	inv	opt	inv	opt
C1-C2	1.739	1.665	-8.61	-11.62	0.46	0.27
C1-O1	1.814	1.712	-6.78	-11.24	0.54	0.47
C2-O1	1.778	1.726	-5.44	-11.72	0.56	0.49
C2-C3	1.807	1.784	-12.88	-15.52	0.16	0.11
C1-C4	1.818	1.744	-13.39	-14.64	0.09	0.09
C3-O2 ^a	3.024	2.936	-33.37	-12.40	0.08	0.13
C3-O3 ^a	2.326	2.066	-27.63	-17.88	0.09	0.03
C4-O4 ^a	2.858	2.833	-31.90	-15.34	0.09	0.12
C4-N1	2.314	2.225	-22.92	-25.70	0.11	0.19
C1-H1	1.925	2.006	-22.16	-27.68	0.05	0.03
C2-H2	1.951	2.006	-22.92	-27.52	0.04	0.03

^a It is known that differences in Laplacian values for polar bonds (here especially carbonyl C-O bonds) can be large between those derived through multipoles and those directly derived from a theoretical wavefunction. This is due to an insufficient flexibility of the radial functions used in the multipole model (A. Volkov, P. Coppens, *Acta Cryst. A*, 2001, **57**, 395-405; J. Henn, D. Ilge, D. Leusser, D. Stalke, B. Engels, *J. Phys. Chem. A*, 2004, **108**, 9442-9452).